

Transmission Electron Microscopic (TEM) analysis of STZ-diabetes induced Cardiac Structural changes in Rats.

C Manikandhan^{1*}, Vivek Daniel¹ and Kratika Daniel²

¹School of Pharmacy, Research department, SunRise University, Alwar-India

²Faculty of Pharmacy, Oriental University, Indore-India

Corresponding author: C Manikandhan, Research scholar, Sunrise University, Alwar, Rajasthan

Received: 17 Jul 2023; Received in revised form: 19 Aug 2023; Accepted: 01 Sep 2023; Available online: 13 Sep 2023

©2023 The Author(s). Published by AI Publications. This is an open access article under the CC BY license

(<https://creativecommons.org/licenses/by/4.0/>)

Abstract— Diabetes mellitus (DM) is a global health crisis, imposing a substantial burden on both healthcare systems and individuals due to its chronic nature and associated complications. Among these complications, cardiovascular diseases rank as the primary cause of morbidity and mortality in people with diabetes. Diabetic cardiomyopathy (DCM), a distinctive form of heart disease, is characterized by structural and functional abnormalities within the heart, independent of conventional cardiovascular risk factors. The multifaceted pathophysiology of DCM involves factors like hyperglycemia-induced oxidative stress, inflammation, altered myocardial metabolism, and fibrosis, collectively leading to cardiac tissue structural changes and impaired function. Streptozotocin (STZ), a compound derived from *Streptomyces achromogenes*, is commonly used to induce diabetes in animal models, particularly rodents, making it a valuable tool for simulating diabetes in laboratory settings. Transmission Electron Microscopy (TEM) provides a powerful means to investigate ultrastructural changes within cardiac tissues at the microscopic level, encompassing myofibrillar structure, mitochondrial integrity, sarcoplasmic reticulum, and interstitial components. Figure-1 illustrates the pathological changes caused by STZ-induced diabetes in experimental animals, showing structural alterations in cardiac and brain tissues. Notably, the use of a polyherbal extract containing *Curcuma amada* rhizome and *Sida spinosa* leaves appears to mitigate some of the detrimental effects of STZ-induced diabetes on cardiac cells, suggesting potential protective benefits.

Keywords— Diabetes Mellitus, Diabetic Cardiomyopathy, Streptozotocin, Transmission Electron Microscopy (TEM), Cardiovascular Complications

I. INTRODUCTION

Diabetes mellitus (DM), a global health epidemic, poses a significant burden on both healthcare systems and individuals due to its chronic nature and associated complications. Among these complications, cardiovascular diseases stand out as the leading cause of morbidity and mortality among individuals with diabetes. Diabetic cardiomyopathy (DCM), a distinct form of heart disease, is characterized by structural and functional abnormalities in the heart, independent of traditional cardiovascular risk factors such as hypertension and atherosclerosis.

The pathophysiology of DCM is multifaceted and includes hyperglycemia-induced oxidative stress, inflammation, altered myocardial metabolism, and fibrosis. These factors collectively contribute to structural changes within the cardiac tissue, ultimately leading to impaired cardiac function.

Streptozotocin (STZ), a naturally occurring compound derived from *Streptomyces achromogenes*, is widely used to induce diabetes in experimental animal models, particularly in rodents. STZ selectively damages pancreatic β -cells, resulting in insulin deficiency and hyperglycemia, making it a suitable tool for simulating

diabetes in laboratory settings.

Transmission Electron Microscopy (TEM) is a powerful imaging technique that allows for the high-resolution visualization of cellular and subcellular structures. In the context of diabetic cardiomyopathy, TEM offers a valuable opportunity to explore and document ultrastructural changes within cardiac tissues at the microscopic level. This includes observing alterations in myofibrillar structure, mitochondrial integrity, sarcoplasmic reticulum, and interstitial components.

The application of TEM analysis in the study of STZ-induced diabetic cardiac structural changes in rats allows for a comprehensive exploration of the ultrastructural alterations within the heart. These findings may provide critical insights into the pathogenesis of diabetic cardiomyopathy and offer valuable information for the development of targeted therapeutic interventions to mitigate cardiac complications in diabetes.

II. RESEARCH METHODOLOGY

The research methodology for conducting Transmission Electron Microscopic (TEM) analysis of STZ-diabetes induced cardiac structural changes in rats involves a systematic approach to sample preparation, imaging, and data analysis. Here is a step-by-step research methodology for your study:

1. Selection of Animal Model:

Choose an appropriate animal model for diabetes induction. Commonly used models include Sprague-Dawley rats.

Confirm diabetes induction using Streptozotocin (STZ) administration, and monitor blood glucose levels to confirm hyperglycemia.

2. Ethical Considerations:

Obtain ethical approval from the relevant institutional animal care and use committee (IACUC) or ethics board for conducting experiments on animals.

Ensure that all procedures adhere to ethical guidelines for animal welfare and humane treatment.

3. Sample Collection and Tissue Preparation:

Sacrifice the rats using approved euthanasia methods and collect cardiac tissue samples.

Fix the cardiac tissue samples in appropriate fixatives (e.g., glutaraldehyde) to preserve ultrastructural

integrity.

Post-fix the samples with osmium tetroxide to enhance contrast for TEM imaging.

4. Tissue Sectioning:

Embed the fixed tissue samples in epoxy resin blocks.

Use an ultramicrotome to cut ultrathin sections (typically around 70-100 nanometers) from the embedded tissue blocks.

Transfer the ultrathin sections onto TEM grids for imaging.

5. TEM Imaging:

Use a transmission electron microscope equipped with an electron beam source to visualize the cardiac tissue sections at high resolution.

Capture TEM images of the cardiac tissue, focusing on areas of interest that may show structural changes, such as myofibrils, mitochondria, and cell membranes.

6. Data Collection and Analysis:

Analyze the TEM images to identify and document ultrastructural changes in the cardiac tissue of diabetic rats. These changes may include:

- Disorganization of myofibrils.
- Mitochondrial abnormalities.
- Changes in sarcoplasmic reticulum morphology.
- Alterations in interstitial components, including collagen and extracellular matrix.
- Quantify the observed changes and compare them with control group data, if applicable.

III. RESULT AND DISCUSSION

Figure-1 Pathological changes caused by STZ-diabetes in the experimental animals are shown by transmission electron microscopy (TEM) analysis of heart sections (Plate (a)–(d)) and brain sections (Figure (2)). Plate a-Group-I shows the usual arrangement of cardiac myocytes in the matrix and serves as a control segment of normal cardiac tissue. The loss of architecture caused by a reduction in cardiac myocyte number and size is seen in Plate b, which depicts cardiac sections from STZ-diabetic mice. STZ-induced hyperglycemia and collagen fibrosis lead to cardiac structural damage, as shown by the arrow. Plate b, shown by the red arrow, displays morphological alterations to the dense nucleus and the concomitant loss of mitochondrial contents. Cardiac

sections from diabetic mice treated with a poly herbal extract of *Curcuma amada* rhizome and *Sida spinosa* leaves are shown in Plate c-Group-III. These mice show a decrease in the loss and atrophy of myocytes due to STZ-diabetes, an increase in collagen fibres, and the preservation of their normal architecture. Plate d-Group-IV poly herbal extract of *Curcuma amada* rhizome

and *Sida spinosa* leaves did not produce any noticeable changes in the patients who received it. Based on the results, we may infer that the poly herbal extract of *Curcuma amada* rhizome and *Sida spinosa* leaves, despite its apparently limited effects, may protect cardiac cells from the cytotoxicity produced by STZ-diabetes.

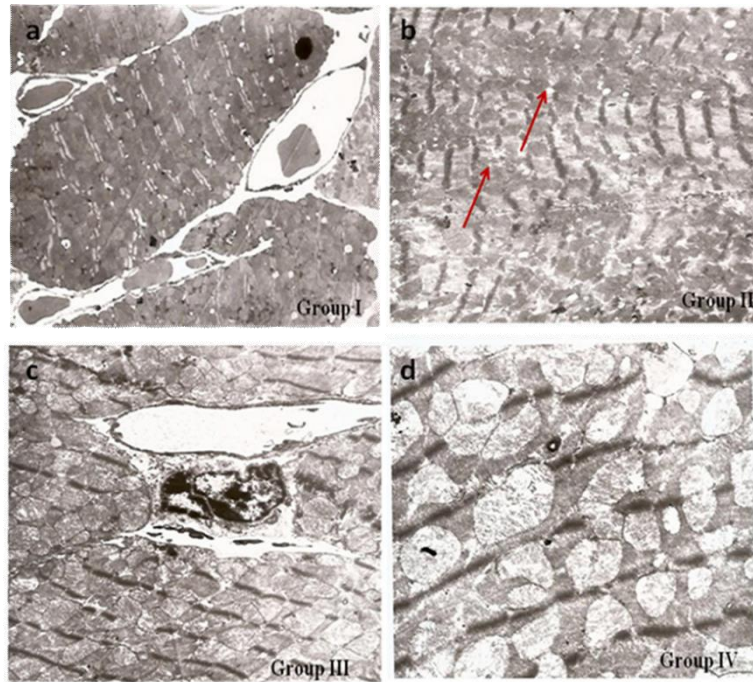


Fig.1: Electron transmission microscopic analysis of cardiac collagen content in control, STZ-induced diabetic, and poly herbal extract of *Curcuma amada* rhizome and *Sida spinosa* leaves treated animals

Animals in Group I (Plate a) served as controls; animals in Group II (Plate b) were used as diabetic controls after receiving STZ; animals in Group III (Plates c and d) received a poly herbal extract of *Curcuma amada* rhizome and *Sida spinosa* leaves; and animals in Group

IV (Plates e and f) received just the poly herbal extract. Mice with diabetes exhibited structural changes and an increase in collagen (shown by the red arrows). Initial growth (by a factor of 5,000).

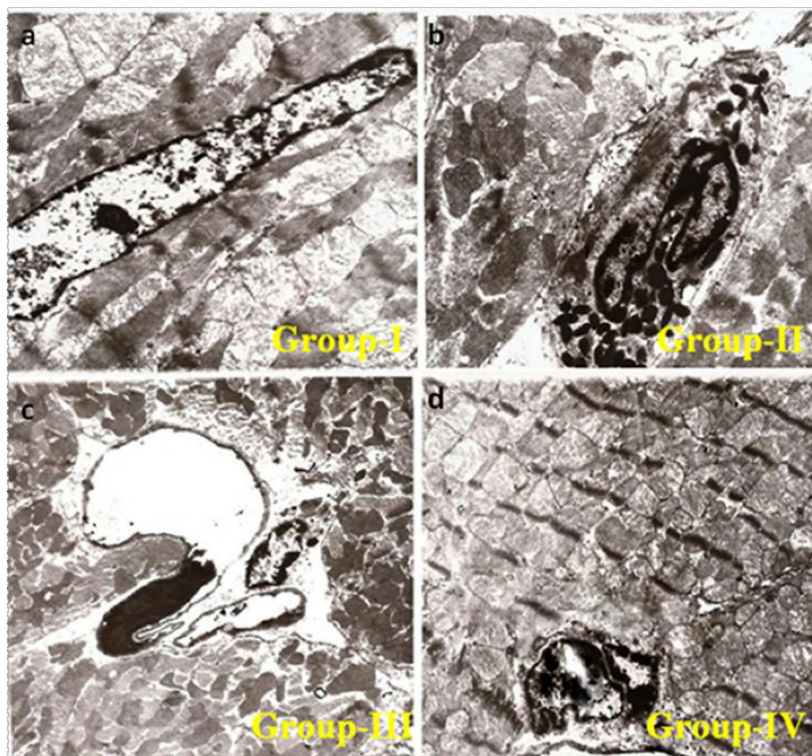


Fig.2: Transmission electron microscopic (TEM) images of cardiac sections in control, STZ-induced diabetic, and poly herbal extract of *Curcuma amada* rhizome and *Sida spinosa* leaves treated animals

Mice that were diabetically induced by streptozotocin (STZ) make up Group II (Plate B), whereas STZ-treated animals and those given a poly herbal extract of

Curcuma amada rhizome and *Sida spinosa* leaves make up Groups III and IV (Plates C and D). Initial growth (by a factor of 5,000).

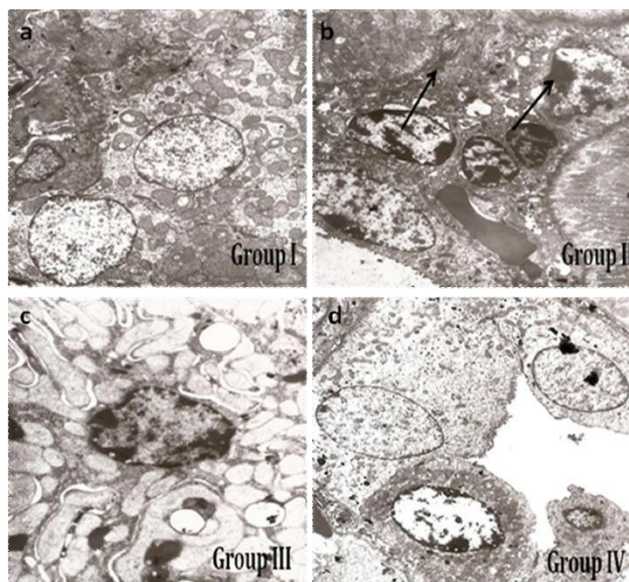


Fig.3: Transmission electron microscopic images of renal sections in control, STZ-induced diabetic, and poly herbal extract of *Curcuma amada* rhizome and *Sida spinosa* leaves treated animals

Mice that were diabetically induced by streptozotocin (STZ)

make up Group II (Plate B), whereas STZ-treated

animals and those given a poly herbal extract of Curcuma amada rhizome and Sida spinosa leaves make up Groups III and IV (Plates C and D). Initial expansion (by a factor of 5,000). Treatment with a polyherbal extract including Curcuma amada rhizome and Sida spinosa leaves restored normal kidney architecture in diabetic mice, as compared to controls. Treatment with a polyherbal extract of Curcuma amada rhizome and Sida spinosa leaves attenuated the progression of glomerulosclerosis and glomerular hypertrophy in rats exposed to STZ, and reversed the effects of STZ on glomerular function. No abnormalities or toxicity signs were seen between normal and group I control mice, which were given a poly herbal extract of Curcuma amada rhizome and Sida spinosa leaves.

Effect of poly herbal extract of Curcuma amada rhizome and Sida spinosa leaves on serum cardiac marker enzymes in the control and experimental group of animals.

Table 1 shows that compared to normal control animals, STZ-diabetic (group II) animals had significantly higher levels of LDH, CPK, CK-MB, and Troponin-I activity (p 0.05), whereas poly herbal extract of Curcuma amada

rhizome and Sida spinosa leaves -treated diabetic mice (group-III) had significantly lower levels of these markers. Curcuma amada rhizome and Sida spinosa leaf polyherbal extract medication control group-IV mice showed no change in LDH, CPK, CK-MB, or Troponin-I activity.

Effect of poly herbal extract of Curcuma amada rhizome and Sida spinosa leaves on serum lipid levels in the control and experimental group of animals.

Table-2 displays the serum cholesterol, TGL, LDL, and HDL values of control-induced and treated animals. Total lipid contents (cholesterol, TGL, and lipoproteins like LDL) increased whereas HDL levels decreased significantly (p 0.05) in STZ-diabetic mice. Changes in the levels of these lipids and lipoproteins strongly reflect abnormal lipid metabolism in STZ-diabetic mice. Poly herbal extract of Curcuma amada rhizome and Sida spinosa leaves normalises total cholesterol, TGL, LDL, and HDL levels in STZ-diabetic mice. There were no discernible changes in the health of animals fed a poly herbal extract of Curcuma amada rhizome and Sida spinosa leaves and those of normal control animals.

Table -1: Serum cardiac marker enzyme levels in the control, STZ-induced diabetic, and poly herbal extract of Curcuma amada rhizome and Sida spinosa leaves treated animals

Groups	LDH	CPK	CK-MB	Troponin-I
Normal control mice (Group-I)	237± 19.31	73.7±6.8	64 ± 6.8	0.60 ± 0.15
STZ-Diabetic mice (Group-II)	462 ±34.47 ^a	146.1±15.4 ^a	146 ± 13.1 ^a	1.32 ±0.17 ^a
STZ-Diabetic mice + PHECASS 100 mg/kg bw (Group-III)	288 ±21.0 ^b	119±3.58 ^b	110 ± 7.6 ^b	0.88 ±0.10 ^b
STZ-Diabetic mice + PHECASS 200 mg/kg bw (Group-IV)	241.9 ±12.4 ^{NS}	78.9±5.12 ^{NS}	72 ± 4.7 ^{NS}	0.64±0.12 ^{NS}

Mean standard deviation (n = 6 mice/group). a = significantly different from Group I at the 0.05 level; b = significantly different from Group II at the 0.05 level; NS = not significant. For LDH, CPK, and CK-MB, the units are IU/L; for troponin-I, the unit is ng/mL.

Table 2: Serum total cholesterol, TGL, LDL and HDL in the control, STZ-induced diabetic, and poly herbal extract of *Curcuma amada* rhizome and *Sida spinosa* leaves treated animal

Groups	Total Cholesterol	Triglycerides	LDL	HDL
Normal control mice (Group-I)	84.40 ± 4.40	55.25 ± 5.11	32.80 ± 2.13	8.90 ± 2.28
STZ-Diabetic mice (Group-II)	198.50 ± 10.20 ^a	130.14 ± 9.52 ^a	89.30 ± 3.73 ^a	14.20 ± 1.29 ^a
STZ-Diabetic mice + PHECASS 100 mg/kg bw (Group-III)	129.34 ± 8.30 ^b	94.20 ± 6.0 ^b	56.25 ± 3.15 ^b	29.14 ± 2.16 ^b
STZ-Diabetic mice + PHECASS 200 mg/kg bw (Group-IV)	90.27 ± 6.11 ^{NS}	58.91 ± 8.24 ^{NS}	35.46 ± 2.3 ^{NS}	35.94 ± 1.95 ^{NS}

Mean standard deviation (n = 6 mice/group). a = significantly different from Group I at the 0.05 level; b = significantly different from Group II at the 0.05 level; NS = not significant. LDL, HDL, and other lipids are measured in milligrammes per millilitre of blood.

Effects of poly herbal extract of *Curcuma amada* rhizome and *Sida spinosa* leaves against diabetes induced lipid accumulation in and STZ-diabetic mice.

Table-3 displays the levels of total lipids (cholesterol, TGL, and phospholipids) in the hearts of the different research groups. Total cardiac lipids, cholesterol, TGL, and phospholipids were all found to be considerably (p

0.05) greater in the STZ-diabetic mice. These cardiac lipids are significantly increased or decreased in STZ-diabetic mice, reflecting the abnormal lipid accumulation in the diabetic heart. Poly herbal extract of *Curcuma amada* rhizome and *Sida spinosa* leaves - treated STZ-diabetic mice had a decrease in cardiac lipid accumulation. There were no discernible changes in the health of animals fed a poly herbal extract of *Curcuma amada* rhizome and *Sida spinosa* leaves and those of normal control animals.

Table-3: Cardiac total lipids, total cholesterol, triglycerides and phospholipids in the control, STZ-induced diabetic, and poly herbal extract of *Curcuma amada* rhizome and *Sida spinosa* leaves treated animals

Groups	Total lipids	Total Cholesterol	Triglycerides	Phospholipids
Normal control mice (Group-I)	20 ± 1.03	2.11 ± 0.10	13.48 ± 0.87	14.52 ± 0.66
STZ-Diabetic mice (Group-II)	38 ± 5.6 ^a	3.98 ± 0.23 ^a	28.89 ± 1.73 ^a	24.75 ± 1.29 ^a
STZ-Diabetic mice + PHECASS 100 mg/kg bw (Group-III)	26 ± 8.30 ^b	2.80 ± 0.15 ^b	20.56 ± 1.35 ^b	18.29 ± 1.08 ^b
STZ-Diabetic mice + PHECASS 200 mg/kg bw (Group-IV)	22 ± 6.11 ^{NS}	2.20 ± 8.24 ^{NS}	12.32 ± 2.3 ^{NS}	13.35 ± 0.98 ^{NS}

Mean standard deviation (n = 6 mice/group). a = significantly different from Group I at the 0.05 level; b = significantly different from Group II at the 0.05 level; NS = not significant. Units are in milligrammes per millilitre.

Effects of poly herbal extract of *Curcuma amada* rhizome and *Sida spinosa* leaves and STZ on the activities of serum and cardiac ATPases.

Table-4 displays the effects on serum and cardiac ATPase activity of a poly herbal extract including *Curcuma amada* rhizome, *Sida spinosa* leaves, and STZ. Reduced enzyme activity in Na⁺/K⁺ ATPase and Ca²⁺ ATPase was seen in STZ-diabetic Group II mice

compared to normal control Group I animals (p<0.05). *Curcuma amada* rhizome and *Sida spinosa* leaves poly herbal extract treatment significantly improved activity levels in STZ-diabetic mice. *Curcuma amada* rhizome and *Sida spinosa* leaf poly herbal extract-treated Group IV animals did not differ significantly from normal control Group I animals.

Table -4: Membrane bound Na⁺/K⁺-ATPase and Ca²⁺-ATPase in the normal control, diabetic control and poly herbal extract of *Curcuma amada* rhizome and *Sida spinosa* leaves treated animals

Groups	Serum Na ⁺ /K ⁺ ATPase	Cardiac Na ⁺ /K ⁺ ATPase	Cardiac Ca ²⁺ ATPase
Normal control mice (Group-I)	0.626 ± 0.006	4.21 ± 0.65	1.93 ± 0.25
STZ-Diabetic mice (Group-II)	0.438 ± 0.024 ^a	2.89 ± 0.32 ^a	0.87 ± 0.10 ^a
STZ-Diabetic mice + PHECASS 100 mg/kg bw (Group-III)	0.560 ± 0.014 ^b	3.84 ± 0.51 ^b	1.68 ± 0.21 ^b
STZ-Diabetic mice + PHECASS 200 mg/kg bw (Group-IV)	0.609 ± 0.010 ^{NS}	4.28 ± 0.60 ^{NS}	1.90 ± 0.26 ^{NS}

Mean standard deviation (n = 6 mice/group). a = significantly different from Group I at the 0.05 level; b = significantly different from Group II at the 0.05 level; NS = not significant. Serum Na⁺/K⁺ ATPase and Na⁺/K⁺ ATPase and Ca²⁺-ATPase values are reported as U/mg protein and mole phosphorus liberated/mg protein/hour, respectively.

Effect of poly herbal extract of *Curcuma amada* rhizome and *Sida spinosa* leaves on STZ-diabetes induced urea and creatinine levels

Figure 3 shows the levels of urea and creatinine in the blood of the test animals. Diabetic mice had substantially elevated urea and creatinine levels compared to normal control animals (p < 0.05). This

marker was significantly reduced in Group IV mice compared to Group III diabetic mice after treatment with a poly herbal extract of *Curcuma amada* rhizome and *Sida spinosa* leaves. The polyherbal extract of *Sida spinosa* leaves and *Curcuma amada* rhizome. The mice in Group II exhibited no significant changes on these measures.

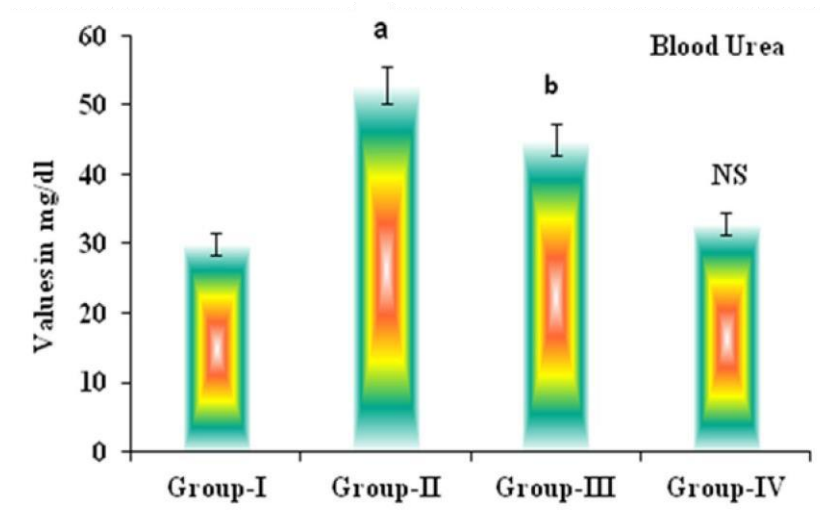


Fig.3: Blood Urea and Creatinine levels in the control, STZ-induced diabetic, and poly herbal extract of *Curcuma amada* rhizome and *Sida spinosa* leaves treated animals

Mean standard deviation (n = 6 mice/group). a = significantly different from Group I at the 0.05 level; b = significantly different from Group II at the 0.05 level; NS = not significant. The standard for measuring urea and creatinine is milligrammes per deciliter.

Effect of poly herbal extract of *Curcuma amada* rhizome and *Sida spinosa* leaves on MDA, NO and endogenous antioxidant levels in experimental groups

Table 3.8 displays the levels of MDA, nitric oxide, and endogenous antioxidants in normal and diabetic mice after administration with a poly herbal extract of *Curcuma amada* rhizome and *Sida spinosa* leaves. Mice in the STZ-induced diabetes group II exhibited significantly higher levels of MDA and NO compared to the normal control group. Group III animals administered with a poly herbal extract of *Curcuma amada* rhizome and *Sida spinosa* leaves had significantly lower levels of reactive oxygen species (ROS) and malondialdehyde (MDA) compared to STZ-induced diabetic mice (group II). No noticeable changes were seen in Group IV- mice that were given just poly herbal extract of *Curcuma amada* rhizome and *Sida spinosa* leaves. Catalase, glutathione peroxidase, and superoxide dismutase are only few of the intracellular antioxidants whose amounts are shown in the table. In comparison to control mice, STZ-induced animals had significantly decreased levels of the antioxidants glutathione (GSH), superoxide dismutase (SOD), and

catalase. Diabetic mice in Group II had significantly lower levels than Group IV animals treated with a poly herbal extract of *Curcuma amada* rhizome and *Sida spinosa* leaves. Mice in group II weren't affected in any noticeable way since they weren't given the drug.

Effects of poly herbal extract of *Curcuma amada* rhizome and *Sida spinosa* leaves and STZ-diabetes induced lipid peroxidation

Streptozotocin (STZ) and a polyherbal extract of *Curcuma amada* rhizome and *Sida spinosa* leaves both produce lipid peroxidation in the blood and heart tissue, as illustrated graphically in Figure-4. The levels of TBARS represented the extent of lipid peroxidation. Group II-STZ diabetic mice had higher levels of TBARS in their serum and heart tissue than the control group. Compared to diabetic mice administered STZ (group-II), TBARS levels were reduced in diabetic animals given a poly herbal extract of *Curcuma amada* rhizome and *Sida spinosa* leaves (group-III). No significant changes were seen between Group-I and Group-IV animals, who were administered a poly herbal extract consisting of *Curcuma amada* rhizome and *Sida spinosa* leaves.

Table-4: MDA, NO and endogenous anti-oxidant levels in the control, STZ-induced diabetic, and poly herbal extract of *Curcuma amada* rhizome and *Sida spinosa* leaves treated animals

Groups	MDA	NO	GSH	SOD (U/mg)	CAT
Normal control mice (Group-I)	74.04 ± 4.98	4.20 ± 0.20	35.53 ± 1.87	27.33 ± 1.19	20.83 ± 1.29
STZ-Diabetic mice (Group-II)	167.9 ± 11.85 ^a	8.36 ± 0.61 ^a	8.36 ± 0.61 ^a	11.89 ± 0.43 ^a	5.73 ± 0.40 ^a
STZ-Diabetic mice + PHECASS 100 mg/kg bw (Group-III)	94.78 ± 6.45 ^b	6.02 ± 0.52 ^b	28.75 ± 1.68 ^b	22.54 ± 0.99 ^b	16.40 ± 0.96 ^b
STZ-Diabetic mice + PHECASS 200 mg/kg bw (Group-IV)	76.89 ± 5.06 ^{NS}	4.85 ± 0.54 ^{NS}	34.48 ± 1.72 NS	26.10 ± 0.85 ^{NS}	9.36 ± 1.11 NS

Mean standard deviation (n = 6 mice/group). a = significantly different from Group I at the 0.05 level; b = significantly different from Group II at the 0.05 level; NS = not significant. Superoxide dismutase (SOD) levels are reported in Units/mg protein; catalase (CAT) levels are reported in micrograms of hydrogen peroxide (H₂O₂) consumed (per minute) per milligramme of protein; glutathione (GSH) levels are reported in micrograms of glutathione (per minute) per milligramme of protein.

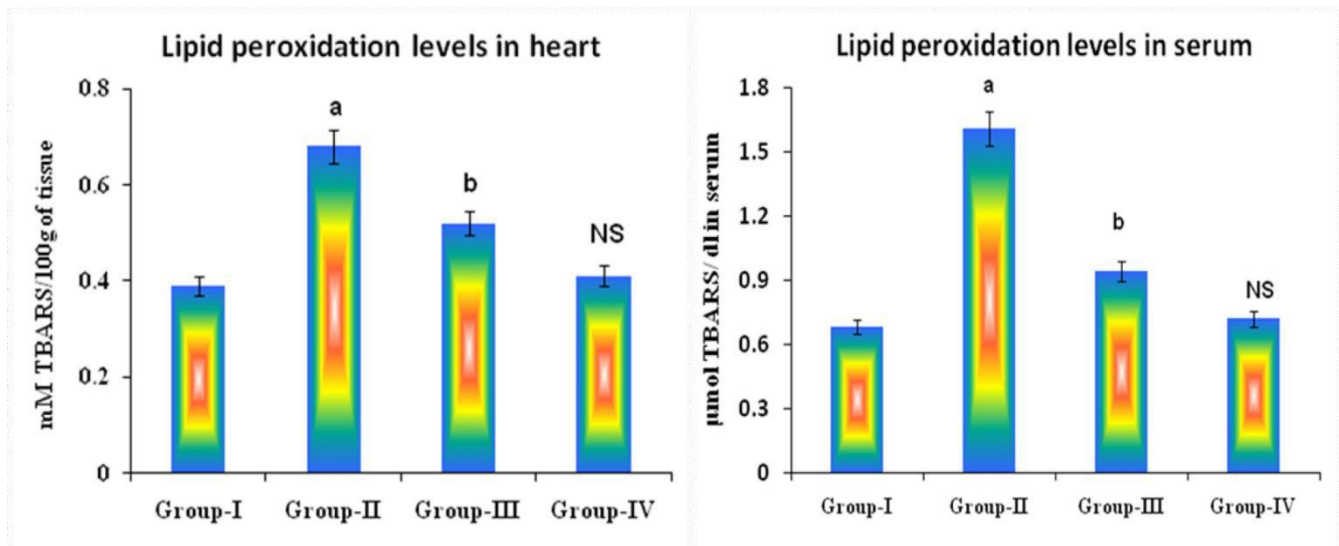


Fig.5: Lipid peroxidation levels in serum and heart tissue in the control, STZ-induced diabetic, and poly herbal extract of *Curcuma amada* rhizome and *Sida spinosa* leaves treated animals

Mean standard deviation (n = 6 mice/group). a = significantly different from Group I at the 0.05 level; b = significantly different from Group II at the 0.05 level; NS

= not significant. Serum TBARS concentrations are reported in nmol/dl, whereas tissue concentrations are reported in millimoles/100 milligrammes.

IV. CONCLUSION

The study, which utilized Transmission Electron Microscopy (TEM) to analyze cardiac structural changes induced by Streptozotocin (STZ)-diabetes in rats, has provided valuable insights into the ultrastructural alterations occurring in diabetic cardiomyopathy. In conclusion, the TEM analysis has elucidated the intricate cardiac structural changes that occur in STZ-induced diabetic rats. These findings underscore the complexity of diabetic cardiomyopathy and its impact on cardiac ultrastructure. Understanding these alterations at the nanoscale level is pivotal for advancing our knowledge of this condition and identifying potential targets for therapeutic interventions. While this study contributes significantly to our understanding of diabetic cardiomyopathy, further research is needed to explore the functional consequences of these ultrastructural changes and to develop targeted treatments aimed at preserving cardiac structure and function in diabetes. Ultimately, this research paves the way for more effective strategies to mitigate the impact of diabetic cardiomyopathy, a critical step toward improving the cardiovascular health of individuals with diabetes.

REFERENCES

- [1] Brunello, E., Fusi, L., Ghisleni, A., Park-Holohan, S., Ovejero, J. G., Narayanan, T., & Irving, M. (2020). Myosin filament-based regulation of the dynamics of contraction in heart muscle. *Proceedings of the National Academy of Sciences, USA*, 117(14), 8177–8186. 10.1073/pnas.1920632117
- [2] Falcão-Pires, I., & Leite-Moreira, A. F. (2012). Diabetic cardiomyopathy: understanding the molecular and cellular basis to progress in diagnosis and treatment. *Heart Failure Reviews*, 17, 325–344. 10.1007/s10741-011-9257-z
- [3] Fenwick, A. J., Awinda, P. O., Yarbrough-Jones, J. A., Eldridge, J. A., Rodgers, B. D., & Tanner, B. C. W. (2019). Demembrated skeletal and cardiac fibers produce less force with altered cross-bridge kinetics in a mouse model for limb-girdle muscular dystrophy 2i. *American Journal of Physiology. Cell Physiology*, 317(2), C226–C234. 10.1152/ajpcell.00524.2018
- [4] Grundy, D. (2015). Principles and standards for reporting animal experiments in *The Journal of Physiology and Experimental Physiology*. *Experimental Physiology* 100(7), 755–758. 10.1113/EP085299
- [5] Guariguata, L., Whiting, D. R., Hambleton, I., Beagley, J., Linnenkamp, U., & Shaw, J. E. (2014). Global estimates of diabetes prevalence for 2013 and projections for 2035. *Diabetes Research and Clinical Practice*, 103, 137–149. 10.1016/j.diabres.2013.11.002
- [6] Han, J. C., Tran, K., Nielsen, P. M., Taberner, A. J., & Loiselle, D. S. (2014). Streptozotocin-induced diabetes prolongs twitch duration without affecting the energetics of isolated ventricular trabeculae. *Cardiovascular Diabetology*, 13, 79–94. 10.1186/1475-2840-13-79
- [7] Huynh, T., Harty, B. J., Claggett, B., Fleg, J. L., McKinlay, S. M., Anand, I. S., Lewis, E. F., Joseph, J., Desai, A. S., Sweitzer, N. K., O'Meara, E., Pitt, B., Pfeffer, M. A., & Rouleau, J. L. (2019). Comparison of outcomes in patients with diabetes mellitus treated with versus without insulin + heart failure with preserved left ventricular ejection fraction (from the TOPCAT Study). *American Journal of Cardiology*, 123, 611–617. 10.1016/j.amjcard.2018.11.022
- [8] Kampourakis, T., & Irving, M. (2015). Phosphorylation of myosin regulatory light chain controls myosin head conformation in cardiac muscle. *Journal of Molecular and Cellular Cardiology*, 85, 199–206. 10.1016/j.yjmcc.2015.06.002
- [9] Krüger, M., Babicz, K., von Frieling-Salewsky, M., & Linke, W. A. (2010). Insulin signaling regulates cardiac titin properties in heart development and diabetic cardiomyopathy. *Journal of Molecular and Cellular Cardiology*, 48(5), 910–916. 10.1016/j.yjmcc.2010.02.012
- [10] Lee, S. I., Patel, M., Jones, C. M., & Narendran, P. (2015). Cardiovascular disease and type 1 diabetes: prevalence, prediction and management in an ageing population. *Therapeutic Advances in Chronic Disease*, 6, 347–374. 10.1177/2040622315598502